Surface Functionalization of Cadmium Sulfide Quantum-Confined Nanoclusters. 3. Formation and Derivatives of a Surface Phenolic Quantum Dot†

Jonathan G. C. Veinot, Madlen Ginzburg, and William J. Pietro*

Department of Chemistry, York University, 4700 Keele St., North York (Toronto), Ontario, Canada, M3J 1P3

Received April 2, 1997. Revised Manuscript Received July 25, 1997⊗

The preparation, characterization, and properties of a novel quantum-confined CdS nanocluster containing a chemically active phenolic surface is described, along with a general method for the covalent attachment of a variety of molecular moieties to the cluster via esterification of the surface hydroxyl groups. The introduction of surface reactivity is crucial for the eventual realization of molecular electronic devices fabricated from such nanoclusters or quantum dots. The esterification method described in this contribution occurs under very mild conditions that have been demonstrated not to disturb the integrity of the cluster and can be extended to include such interesting moieties as chromophores, luminophores, or quantum wires. Interestingly, tethering aliphatic chains of moderate length to a CdS nanocluster renders the cluster soluble in a wide variety of common laboratory solvents. Thus, surface phenolic semiconductor nanoclusters can serve as a convenient synthetic starting point for a wide variety of interesting and potentially applicable composite materials.

Introduction

Nanometer diameter semiconductor clusters, or quantum dots, are currently the focus of much intensive research.[1] These fascinating systems exhibit optical and electronic properties quite different from their corresponding bulk semiconductor materials, due primarily to phenomena arising from quantum confinement effects, and may eventually form the basis of new and unusual molecular electronic devices.[2] The realization of such devices may well occur via structural coupling through surface functionalities. Thus, the creation of a few surface-functionalized semiconductor nanocrystallites has recently been reported,[3−5] and we have previously reported the synthesis and physical and chemical properties of novel cadmium sulfide quantum-confined nanoclusters baring chemically active surface pyridyl functionalities[6] by way of a modification of a previously described kinetic trapping technique.[7] Indeed, the use of surface functionalities to form macromolecular aggregates of discrete semiconductor nanoclusters is already underway.[8] We report here the creation of a CdS nanocluster having a chemically active phenolic surface (**1**, QDOH) and describe a versatile method for tethering a variety of molecular moieties to the quantum dot through esterification of the phenolic group (the product nanoclusters will be referred to as $QDCO_2R$, **2**).

Experimental Section

Chemicals. Reagent grade toluene was dried over 4 Å molecular sieves and filtered prior to use. Dimethyl sulfoxide (DMSO) was purchased from Aldrich ACS spectrophotometric grade and used without further purification. Water was first deionized by passage through a Sybron-Barnstead D8902 mixed-bed ion-exchange column and then freed from organic impurities using a Sybron-Barnstead D8204 activated charcoal filter. All deuterated solvents used for ^{1}H NMR spectroscopy were purchased in sealed ampules from Cambridge Isotope Laboratories (Andover, MA) and used immediately upon opening the ampule. Sodium sulfide nonahydrate, imidazole, 1-pyrenecarboxylic acid, *n*-butanoyl chloride, decanoyl chloride, and thionyl chloride were purchased reagent grade from Aldrich and used as supplied. Acetic anhydride, butyric anhydride, and benzoyl chloride were obtained reagent grade from BDH and used without further purification. Cadmium acetate (Aldrich reagent grade) was recrystallized from glacial acetic acid and dried at 100 °C in vacuo. 4-Hydroxythiophenol was obtained reagent grade from Aldrich and distilled under reduced pressure immediately prior to use.

Preparation of Surface Phenolic CdS Quantum Dot (QDOH). Sodium sulfide nonahydrate (2.53 g, 11 mmol) and 4-hydroxythiophenol (4.93 g, 39 mmol) were dissolved in 150 mL of a 1:1:2 (v/v) acetonitrile/methanol/water solvent mixture and added to a rapidly stirring solution of 5.05 g (29 mmol) cadmium acetate in the same solvent system under nitrogen. The reaction mixture was protected from light and stirred under nitrogen for 12 h, during which time a bright yellow precipitate formed. The solution was concentrated to about

† For part 2 in this series see ref 8b.

⊗ Abstract published in *Advance ACS Abstracts,* September 1, 1997.

(1) For recent reviews see: (a) Alivisatos, A. P. *J. Phys. Chem.* **1996**, *100*, 13266. (b) Weller, H. *Angew. Chem., Int. Ed. Engl.* **1993**, *32*, 41. (c) Schmid, G. *Chem. Rev.* **1992**, *92*, 1709. (d) Steigerwald, M. L.; Brus, L. E. *Acc. Chem. Res.* **1990**, *23*, 183. (e) Henglein, A. *Chem. Rev.* **1989**, *89*, 1861.

(2) (a) Merkt, U.; Sikorski, Ch. *Semiconduct. Sci. Technol.* **1990**, *5*, 182. (b) Fulton, T. A. *Nature* **1988**, *346*, 408. (c) Zorman, B.; Ramakrishna, M. V.; Friesner, R. A. *J. Phys. Chem.* **1995**, *99*, 7649.

(3) Torimoto, T.; Maeda, K.; Maenaka, J.; Yoneyama, H. *J. Phys. Chem.* **1994**, *98*, 13658.

(4) Nosaka, Y.; Ohta, N.; Fukuyama, T.; Fujii, N. *J. Colloid Interface Sci.* **1993**, *155*, 23.

(5) Torimoto, T.; Uchida, H.; Sakata, T.; Mori, H.; Yoneyama, H. *J. Am. Chem. Soc.* **1993**, *115*, 1874.

(6) Noglik, H.; Pietro, W. J. *Chem. Mater.* **1994**, *6*, 1593.

(7) Herron, N.; Wang, Y.; Eckert, H. *J. Am. Chem. Soc.* **1990**, *112*, 1322.

(8) (a) Peng, X.; Wilson, T. E.; Alivisatos, A. P.; Schultz, P. G. *Angew. Chem., Int. Ed. Engl.* **1997**, *36*, 145. (b) Noglik, H.; Pietro, W. J. *Chem. Mater.* **1995**, *7*, 1333. (c) Lawless, D.; Kapoor, S.; Meisel, D. *J. Phys. Chem.* **1995**, *99*, 10392. (d) Brust, M.; Bethell, D.; Schiffrin, D. J.; Kiely, C. J. *Adv. Mater.* **1995**, *7*, 795. (e) Majetich, S. A.; Carter, A. C.; McCulough, R. D.; Seth, J.; Belot, J. A. *Z. Phys. D* **1993**, *26*, 210.

S0897-4756(97)00189-0 CCC: $14.00

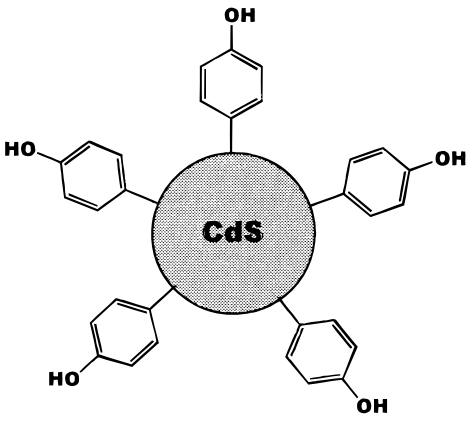

1, QDOH

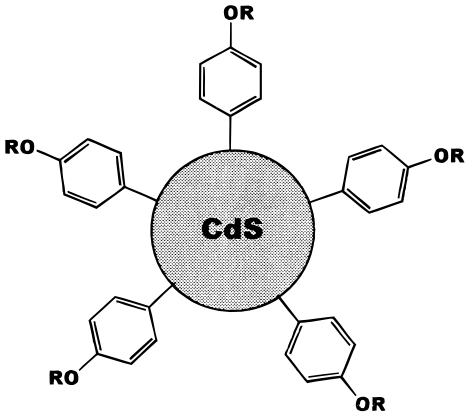

2, $QDCO_2R$; -COR = (a) $-COCH_3$, (b) $-COCH_2CH_2CH_3$,

(c) 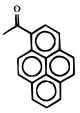 , (d) -COϕ, (e) $-COC_9H_{19}$

one-third its original volume using a rotary evaporator, and the solid was isolated by centrifugation. The solid was purified by repeated washing/sonication/centrifugation cycles with, sequentially, water, acetone, and finally ether, and then dried in high vacuum overnight at room temperature. Yield: 2.23 g (assuming that the yield based on sulfide is quantitative, this would imply that 20 mol % of the cluster's sulfur comes from thiol). Sonication of a sample of this yellow powder in DMSO yielded a transparent suspension that appeared completely nonopalescent under ambient room light but exhibited a pronounced Tyndall effect when directly exposed to the beam of a He−Ne laser. ^{1}H NMR (DMSO) δ 6.0−7.3 (m, 4H), 8.6−9.1 (m, 1H D_2O exchangeable); IR (KBr, cm^{-1}) 3302 (s, br, OH), 1870, 1734 (w, ring overtone), 819 (s, ring CH); UV−vis (nm) 295 (edge), 305 (shldr).

1-Pyrenecarboxylic Acid Chloride. 1-Pyrenecarboxylic acid (1.0 g, 4.1 mmol) was dissolved in 20 mL of thionyl chloride under a dry nitrogen atmosphere. The solution was stirred at room temperature for several minutes, during which time an olive green precipitate formed. The reaction mixture was then heated to 80 °C for 3 h (the green precipitate redissolved), cooled, and filtered. The excess thionyl chloride was removed completely from the filtrate in vacuo to yield 1-pyrenecarboxylic acid chloride as a highly fluorescent orange-yellow solid, which was immediately used to prepare *N*-pyrene-1-carboxoylimidazole (**3c**) as described below.

***N*-Acylimidazoles.** *N*-Acetylimidazole and *N*-butanoylimidazole were prepared by dissolving imidazole in a large excess of the corresponding acid anhydride and stirring for 30 min under a dry nitrogen atmosphere at room temperature. Removal of the liquid (which consisted of acid and excess anhydride) under reduced pressure afforded white crystals, which were recrystallized from toluene. All other *N*-acylimidazoles were prepared as follows. A 50% solution of the corresponding acyl chloride in dry toluene was added dropwise with rapid stirring to a toluene solution of 2.05 equivalents of imidazole at room temperature, heated to 100 °C, and the white precipitate (identified as imidazole hydrochloride) was hot filtered. Cooling the toluene solution in an ice bath resulted in the precipitation of white crystals of the appropriate *N*-acylimidazole, which was recrystallized once from toluene prior to use. Yields and spectroscopic data for all *N*-acylimidazoles prepared in this work are presented in Table 1.

Esterification of Surface Phenol Functionalized CdS Quantum Dots. All esterification reactions were carried out under similar conditions; the procedure for the preparation of the acetyl ester of QDOH is described here as a representative example. To a sonicated suspension of 300 mg of QDOH in 5 mL of DMSO, 5 mL of a solution containing 170 mg of acetylimidazole in DMSO was added dropwise with rapid stirring in the dark under an atmosphere of dry nitrogen, and the mixture was stirred for 30 min at room temperature. The reaction mixture was then cooled in an ice bath and quenched with water. The resulting precipitate was isolated by centrifugation, sonicated repeatedly (and consecutively) in water, methanol, acetone, and ether, and dried in high vacuum at room temperature for 24 h. Reaction conditions, conversion ratios, and spectroscopic data for all $QDCO_2R$ nanocluster esters prepared in this work are presented in Tables 1−3.

Spectroscopy. Infrared spectra were recorded as KBr pellets with a Mattson 3000 Fourier Transform infrared spectrometer. ^{1}H NMR spectra were performed on a Brucker ARX 400 MHz Nuclear Magnetic Resonance Spectrometer using DMSO-d_6 as a solvent for QDOH and all $QDCO_2R$ clusters except **2e** (R = decanoyl), for which $CDCl_3$ was used. Electronic spectroscopy on all quantum dot esters were performed in chloroform (methanol was used for QDOH) in 1 cm quartz cuvettes using a Hewlett-Packard 8452 diode array spectrophotometer.

Electron Microscopy. Transmission electron microscopy (TEM) was performed using a Philips EM-301 transmission electron microscope. Nanocluster samples for TEM analysis were prepared by applying three drops of a freshly sonicated and centrifuged chloroform suspension of the nanocluster (2.5 mg of nanocluster to 3 mL of $CHCl_3$) onto J. B. EM Services (Pointe Claire, Dorval, Que.) JBS-183 300 mesh carbon-coated copper grids (cleaned in acetone, then chloroform, then acetone, and air-dried). The solvent was absorbed through the grid by a layer of filter paper, leaving aggregates as well as individual nanoclusters adhering to the grid wires. The grids were then air-dried at room temperature. Size calibration was performed using a precision silicon grid of 21 600 lines cm^{-1}.

Results and Discussion

The realization of optical or electronic devices employing quantum-confined nanoclusters will ultimately involve the coupling of molecular moieties, such as chromophores, luminophores, molecular wires, or redox centers, to a chemically activated nanocluster surface. Maintaining the integrity of thiophenolate-trapped CdS semiconductor nanoclusters while covalently tethering interesting molecules to the surface of these macromolecular systems does, however, pose a serious problem.[6] The cluster−cadmium/thiolate bond is relatively unstable under many common synthetic conditions (such as in moderately acidic or basic solutions), the clusters are thermally labile, the propensity for thiophenolates to form disulfides renders the clusters unstable to oxidizing conditions, and the sulfur site may exhibit competing reactivity toward reagents intended for the surface functionality. Indeed, the acidic conditions required for a straightforward Fischer−Speier esterifi-

Table 1. Reaction Conditions, Yields, and 400 MHz ^{1}H FT NMR Data

compd	solvent, rxn time	yield or conversion (%)	δ (ppm)
1	$CH_3CN/CH_3OH/H_2O$, 12 h		6.0−7.3 (m, 4H, arom), 8.6−9.1 (m, 1H, −OH)
2a	DMSO, 30 min	95	6.0−7.7 (m, 4H, arom), 2.2 (s, 3H, $-CH_3$)
2b	DMSO, 30 min	97	6.0−7.7 (m, 4H, arom), 2.5 (br, 2H, α-CH_2), 1.6 (br, 2H, β-CH_2), 0.95 (br, 3H, $-CH_3$)
2c	DMSO, 30 min	95	6.4−9.5 (m, arom)
2d	DMSO, 30 min	100	6.4−8.2 (m, arom)
2e	DMSO, 30 min	100	6.4−7.3 (m, 4H, arom), 2.5 (br, 2H, α-CH_2), 1.7 (br, 2H, β-CH_2), 1.2−1.5 (br, 12H, aliph), 0.91 (br, 3H, $-CH_3$)
3a	$(CH_3CO)_2O$, 30 min	100	8.4 (s, 1H, ImC_2), 7.7 (s, 1H, ImC_4), 7.1 (s, 1H, ImC_5), 2.2 (s, 3H, $-CH_3$)
3b	$(n\text{-}PrCO)_2O$, 15 min	50	8.4 (s, 1H, ImC_2), 7.7 (s, 1H, ImC_4), 7.1 (s, 1H, ImC_5), 3.1 (t, 2H, α-CH_2), 1.8 (m, 2H, β-CH_2), 1.0 (t, 3H, $-CH_3$)
3c	ϕCH_3, 30 min	65	8.2−8.5 (m, 10H, ImC_2+pyrene), 7.8 (s, 1H, ImC_4), 7.2 (s, 1H, ImC_5)
3d	ϕCH_3, 15 min	100	8.2 (s, 1H, ImC_2), 7.7 (s, 1H, ImC_4), 7.2 (s, 1H, ImC_5), 7.8 (d, 2H, ϕ2,6), 7.6 (m, 2H, ϕ3,5), 7.7 (s, 1H, ϕ4), 2.6 (s, 3H, $-CH_3$)
3e	ϕCH_3, 30 min	100	8.4 (s, 1H, ImC_2), 7.7 (s, 1H, ImC_4), 7.0 (s, 1H, ImC_5), 3.0 (t, 2H, α-CH_2), 1.7 (m, 2H, β-CH_2), 1.2−1.4 (br, 12H, aliph), 0.9 (t, 3H, $-CH_3$)

Table 2. FT IR Data[a] of Functionalized CdS Nanoclusters as KBr Pellets

cluster	wavenumbers (cm^{-1})
1	3301 (s, v br, O−H str), 1870 and 1730 (w, 1,4-disub -ϕ- overtone), 1636 (m), 1598 (s), 1488 (s, ring C═C), 1429 (s), 1359 (m), 1170 (s, br, ϕ−O), 1088 (m), 1009 (m, ϕ−S), 819 (s, ϕC−H out-of-plane), 634 (m), 510 (m)
2a	3400 (w, v br, residual −OH), 3060 (w, arom C−H str), 2931 (w, aliph C−H str), 1486 (s, ring C═C), 1758 (vs C═O str), 1582 (w), 1427 (w), 1369 (s), 1223 (s, br, ϕ−O), 1085 (m), 1013 (s, ϕ−S), 911 (w), 840 (m), 820 (m, ϕC−H out-of-plane), 797 (w), 510 (m)
2b	3375 (vw, vbr, residual −OH), 3090 (w, arom C−H str), 2965 (m, br, aliph C−H str), 2934 (w, shldr, aliph C−H str), 2875 (w, aliph C−H str), 1751 (vs, C═O str), 1580 (vw), 1539 (vw), 1485 (vs, ring C═C), 1245−1203 (vs, br, ϕ−O), 1167 (vs), 1080 (m), 1013 (m, ϕ−S), 836 (w, ϕC−H out-of-plane), 749 (vw), 653 (vw), 510 (w)
2c	3129, 3047, and 2973 (w, arom C−H str), 1720 (s, C═O str), 1583 (m), 1490 (vs, ring C═C), 1364 (m), 1234 (s, br, ϕ−O), 1205 (shldr), 1167 (shldr), 1066 (m), 842 (s), 818 (s, ϕC−H out-of-plane), 748 (w), 712 (w), 645 (w), 511 (w)
2d	3400 (vw, vbr, residual −OH), 3060 and 3033 (w, arom C−H str), 1736 (vs, C═O str), 1673 (m), 1600 (w), 1485 (s, ring C═C), 1451 (m), 1269 (vs, br, ϕ−O), 1201 (vs), 1166 (s, shldr), 1061 (s), 1013 (m, ϕ−S), 902 (w), 876 (w), 822 (w, ϕC−H out-of-plane), 705 and 686 (vs, shrp, monosub ϕC−H out-of-plane), 634 (vw), 511 (m)
2e	3060 (vw, arom C−H str), 2925 (s, aliph C−H str), 2852 (s, br, aliph C−H str), 1754 (s, C═O str), 1579 (w), 1537 (w), 1486 (s, ring C═C), 1458 (m), 1377 (w), 1170−1081 (s, br, many bands), 1012 (m, ϕ−S), 915 (w), 840−802 (w, br), 736 (vw), 510 (m)

[a] Legend: vs very strong, s strong, m medium, w weak, vw very weak, vbr very broad, br broad, shrp sharp, shldr shoulder, arom aromatic, aliph aliphatic.

Table 3. UV−Visible Absorptions, Calculated (Eq 1) and Measured (TEM) Cluster Diameters

cluster	λ[a] (nm)	calcd diam[b] (Å)	measd diam[c] (Å)
1	390	24	30.4
2a	400	25	27.3
2b	420	27	24.7
2c	356−420 (pyrene $\pi-\pi^*$)		26.3
2d	350	19	28.2
2e	420	27	28.2

[a] CdS band-to-band absorption unless otherwise noted. [b] Tight-binding band theory.[13] [c] Transmission electron microscopy.

cation would certainly destroy the cluster, as did our initial attempts to esterify using acyl chlorides. Our strategy here for further modification of the phenolic surface of QDOH involves ester formation using the family of *N*-acylimidazoles, a popular class of reagents used for the tagging of tyrosine residues,[9] as outlined in Scheme 1. *N*-Acylimidazoles are easily prepared from readily available starting materials, are only slightly air sensitive, and are capable of high-yield esterification of phenols under mild conditions. We found that this reagent family is successful for the creation of a wide variety of $QDCO_2R$ esters from QDOH without significant loss of cluster integrity due to thioester formation.

QDOH nanoclusters are conveniently prepared by a modification of a well-known kinetic trapping method,

Scheme 1

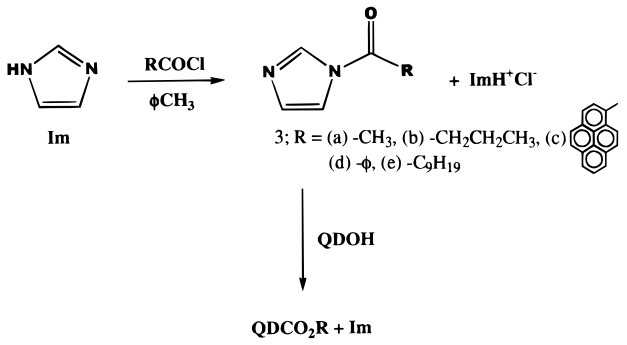

as has been previously described.[6] Like their unfunctionalized thiophenol-capped counterparts,[7] the QDOH nanoclusters are insoluble in water, ether, and hexane, and "soluble" in DMSO and DMF;[10] however, the QDOH clusters are also soluble in methanol and ethanol, presumably due to hydrogen-bonding interactions with the phenolic surface. Assuming quantitative yield based on the limiting precipitant (sulfide), and ascribing additional mass above theoretical yield to thiophenolate cap, the yield data imply that 34 mol % of the total sulfur is contributed by capping thiol. Assuming a

(9) (a) Kronman, M. J.; Holmes, L. O.; Robbins, F. M. *J. Biol. Chem.* **1971**, *246*, 1909. (b) Hirayama, O.; Matsuda, H.; Takeda, H.; Maenaka, H.; Takatsuka, H. *Biochem. Biophys. Acta* **1975**, *384*, 127.

(10) By "soluble" we indicate that the clusters form clear transparent suspensions which appear nonopalescent by ambient illumination, do not settle, and cannot be separated by conventional centrifugation, but however do exhibit a pronounced Tyndall effect when directly illuminated with the beam of a laser.

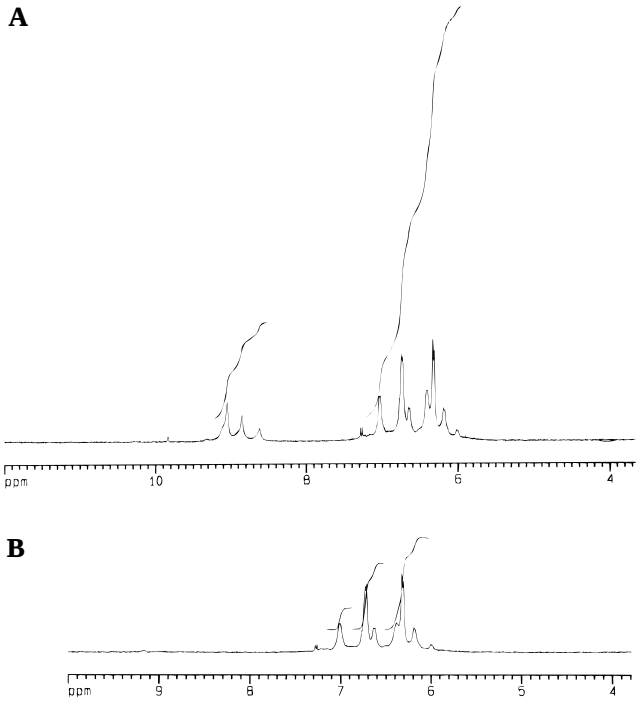

Figure 1. (a) The 400 MHz ^{1}H NMR spectrum of QDOH in DMSO-d_6. (b) After addition of one drop of D_2O.

specific gravity of 4.8 for the CdS core, these data estimate about 130 caps/30 Å diameter nanocluster, which translates to an average surface coverage of 22 Å^2/cap (a 30 Å diameter sphere has a surface area of 2827 Å^2). Applying this approach to previously reported elemental analysis data for unfunctionalized[7] and pyridine functionalized[6] thiophenolate-capped CdS nanoclusters prepared by kinetic trapping yields average surface coverages of 25 and 22 Å^2/cap, respectively, in very good agreement with the gravimetric results presented here.

The ^{1}H NMR spectrum of QDOH in DMSO is presented in Figure 1a. All cluster signals appear somewhat homogeneously broadened, as has been previously observed with 20 Å unfunctionalized thiophenol-capped CdS nanoclusters,[11] 4-hydroxythiophenol-capped PbS microcrystals,[5] and *n*-butanethiolate-capped CdSe systems.[12] No signals were observed upfield of 5 ppm, except for solvent residuals and a sharp singlet due to a small amount of water, possibly chemisorbed at the cluster surface. The broad but structured aromatic resonances between 6.0 and 7.3 ppm are indicative of ring protons in multiple environments, as is the hydroxyl proton resonance between 8.6 and 9.1 ppm. Nevertheless, the integration ratio is, as expected, precisely four to one. The resonance at 8.6−9.1 ppm completely vanishes upon the addition of a drop of D_2O to the DMSO suspension, providing further support for our assignment (Figure 1b).

The infrared spectrum of QDOH shows the characteristic benzene ring C═C (1488 cm^{-1}) and overtone and combination bands (1870 and 1734 cm^{-1}) indicative of a 1,4-disubstitution pattern, as well as the single sharp C−H out-of-plane wag (again characteristic of a 1,4-disubstituted benzene ring) at 819 cm^{-1}. This is in strong contrast with the IR spectrum of the unfunctionalized thiophenol-capped CdS nanocluster which exhibits the two very strong sharp absorptions at 686 and 734 cm^{-1} expected of a monosubstitued benzene derivative, along with the characteristic weak four-band overtone pattern between 1730 and 1950 cm^{-1}. However the most characteristic features of the phenolic functionality are the broad intense O−H stretching vibration centered at 3301 cm^{-1} and the medium-intensity ϕO−H deformation band at 1013 cm^{-1}. In addition, the QDOH nanoclusters, like their unfunctionalized counterparts, show no sign of characteristic ϕS−H stretch at ca. 2580 cm^{-1} (typically a moderately strong band), affording further evidence that the capping agent is entirely sulfur-bound thiolate.

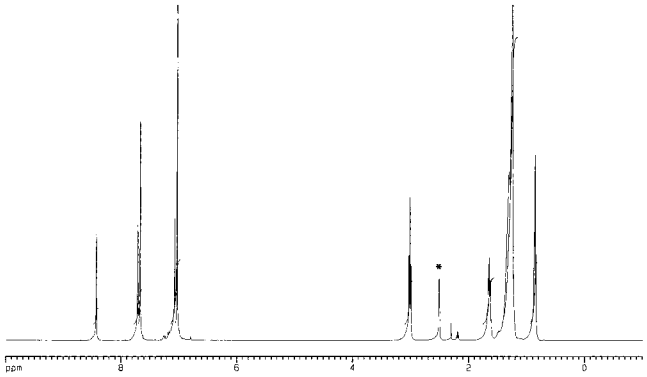

Figure 2. The 400 MHz ^{1}H NMR spectrum of N-decanoylimidazole in DMSO-d_6. ∗ indicates DMSO residual signal.

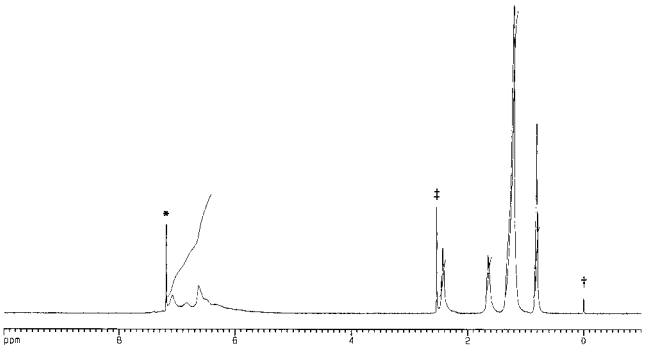

Figure 3. The 400 MHz ^{1}H NMR spectrum of the decanoyl ester of QDOH, **2e** in $CDCl_3$. ∗ indicates chloroform residual signal, ‡ indicates water, and † indicates TMS.

The *N*-acylimidazoles are most conveniently prepared by reacting the corresponding acyl chloride with 2 equiv of imidazole. The *N*-acylated cation is in all cases a stronger acid than the conjugate acid of unsubstituted imidazole; hence, the second equivalent of imidazole precipitates out HCl. *N*-Acylimidazoles can alternatively be prepared from the corresponding acid anhydride. Acyl group transfer to QDOH is carried out at room temperature in dilute DMSO solution under an inert atmosphere. Esterification is usually complete within 15−30 min. Table 1 presents the yields and ^{1}H NMR data for *N*-acylimidazoles **3a**−**e**, along with the reaction conditions, yields (as percent of esterified phenol groups), and ^{1}H NMR data for the corresponding quantum dot esters, QDCO$_2$R, **2a**−**e**. Tables 2 and 3 contain the infrared absorption and electronic spectra, respectively, for **2a**−**e**. Figure 2 shows the ^{1}H NMR spectrum of **3e**. The assignments of **3a**−**e** are straight-

(11) Sachleben, J. R.; Wooten, E. W.; Emsley, L.; Pines, A.; Colvin, V. L.; Alivisatos, A. P. *Chem. Phys. Lett.* **1992**, *198*, 431.
(12) Majetich, S. A.; Carter, A. C.; Belot, J.; McCullough, R. D. *J. Phys. Chem.* **1994**, *98*, 13705.

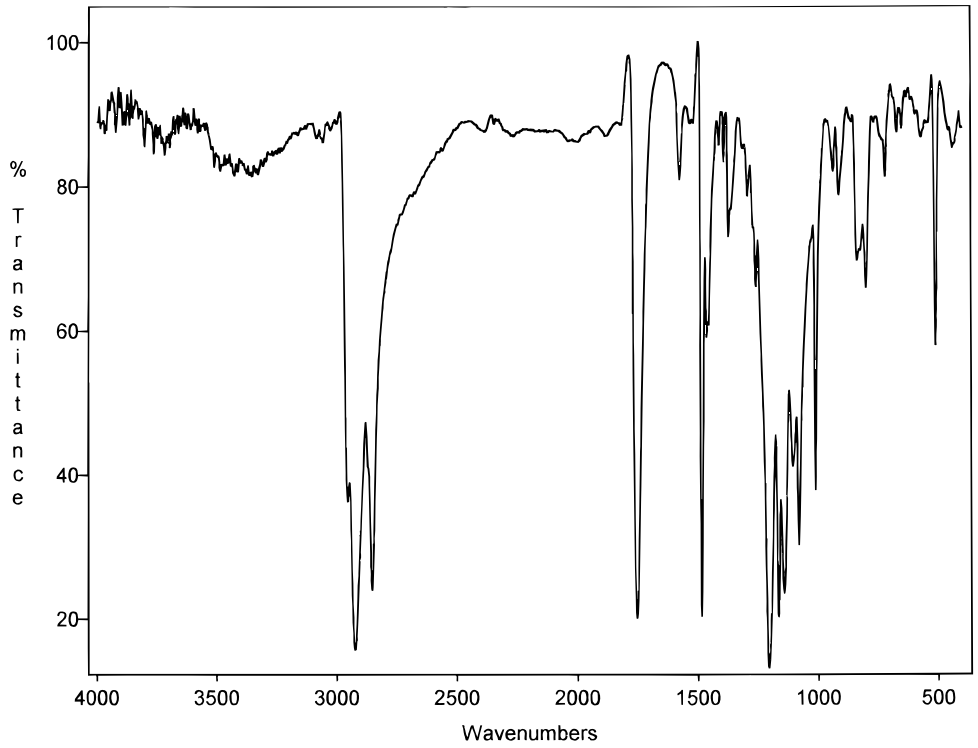

Figure 4. Infrared absorption spectrum of the decanoyl ester of QDOH, **2e**, in KBr.

forward; the imidazole ring resonances appear in all cases at ca. δ 7.0 (s, C_4, 1H), 7.7 (s, C_5, 1H), and 8.4 (s, C_2, 1H), and the acyl group resonances are tabulated in Table 1. The ^{1}H NMR spectra of the esterified clusters **2a**−**e** all exhibit a similar feature in the aromatic region of a broad signal with defined structure superimposed on it (see Figure 3). In some cases small amounts of phenolic −OH resonance were observed, indicating incomplete esterification. The degrees of esterification (reported as percent conversions) recorded in Table 1 were estimated from the integration ratio of the residual −OH signals to the aromatic protons. Control experiments perfomed using unfunctionalized thiophenol-capped CdS nanoclusters showed no reaction with *N*-acylimidazoles (aqueous workup afforded only unchanged nanocluster and recovered organic acid), eliminating the possibility of chemisorption to the CdS core.

Figure 4 shows a typical $QDCO_2R$ infrared absorption spectrum. In all cases, the spectra exhibit ring modes and para-disubstituted C−H out-of-plane vibrations similar to those observed in QDOH, although the overtone and combination bands are generally too weak to discern. Also, in all cases, esterification gives rise to the appearance of the expected carbonyl stretching vibration at ca. 1750 cm^{-1}, and a marked decrease, but not always complete elimination, of the O−H stretch at ca. 3300 cm^{-1}, again suggesting incomplete esterification (typically 95−100%). Extending the reaction time does not appear to afford any greater degree of esterification, and prolonged exposure of QDOH to the reaction conditions (>12 h) results in destruction of the cluster with concomitant precipitation of bulk CdS, and isolation of a crystalline organic compound that we identified as the corresponding O,S-diester. All $QDCO_2R$ esters are also characterized by a weak-to-medium intensity sharp band at ca. 1015 cm^{-1} and a strong broad absorption centered at about 1200−1270 cm^{-1},

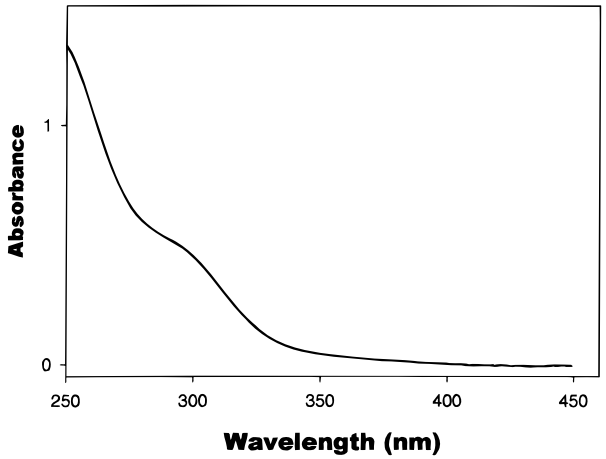

Figure 5. Optical absorption spectrum of 10^{-4} M QDOH in methanol (1 cm path length).

which were assigned to an S-coupled ring mode and phenyl−O antisymmetric stretch, respectively (the former band also appears in the unfunctionalized thiophenol-capped CdS cluster and in QDOH). For clusters **2c** and **2d** the carbonyl stretching frequency appears considerably lower (1720 and 1736 cm^{-1}, respectively) relative to their aliphatic counterparts, suggesting that the aromatic groups are resonance coupled to the carbonyl. IR absorption band assignments for **2a**−**e** are summarized in Table 2.

The electronic absorption spectrum of a QDOH suspension in methanol is presented in Figure 5 and is typical of a thiolate-capped CdS quantum-confined nanocluster[7] with the onset of band-to-band absorption at ca. 390 nm, affording a bandgap of 3.19 eV. The difference of 0.66 eV between the bandgap of QDOH and that of bulk CdS ($E_g(4) = 2.53$ eV) arises from carrier quantum confinment effects and can be used to estimate a diameter of 24 Å for the QDOH cluster in accordance

with recent tight-binding band analyses.[13] This value is in good agreement with the diameters of unfunctionalized and pyridyl functionalized CdS nanoclusters prepared under similar conditions (ca. 20 Å).[6−8,11,12] Upon esterification the situation does not change. The optical absorption spectra for **2a**−**e**, like QDOH, are typical for thiolate-capped CdS nanoclusters. Cluster diameters calculated from the electronic spectra demonstrate that in all cases (except **2c**) the diameter of $QDCO_2R$ is identical with that of the starting QDOH nanocluster, indicating that esterification does not result in removal of capping agent with concomintant cluster fusion. For cluster **2c** the diameter could not be determined by this method because the very intense pyrene $\pi-\pi^*$ transitions mask the CdS absorption. These data are collected in Table 3.

Transmission electron microscopy (TEM) of QDOH and all of the $QDCO_2R$ esters studied in this contribution demonstrate that the nanoclusters tend to agglomerate into larger spheroids of various sizes imbedded in fields of individual nanoclusters. Such behavior is typical of capped metal sulfide nanoclusters.[6,8] Histogram analyses indicate a fairly monodisperse nanocluster diameter of ca. 30.4 ± 7^{15} Å for QDOH, in excellent agreement with the size estimation by electronic spectroscopy. Nanocluster size data by electron microscopy are also tabulated in Table 3, and Figure 6 shows a typical electron micrograph of a large aggregate (1100 Å) with surrounding individual nanoclusters.

Finally, the solubility properties of the $QDCO_2R$ esters are noteworthy. While the QDOH clusters are soluble in lower alcohols, the esterified clusters are not, in support of the notion that the alcohol solubility of QDOH results from hydrogen-bonding interactions between the solvent and the cluster's phenolic surface. On the other hand, solubility in acetone and diethyl ether increases with increasing aliphatic chain length, viz, the decanoyl ester is soluble in ether, and the butanoyl and decanoyl esters are soluble in acetone, whereas the benzoyl and acetyl esters are insoluble in both solvents. Solubility in DMSO appears to vanish for esters having very long aliphatic chains (i.e., the decanoyl ester), and all esters **2a**−**e** are soluble in chloroform, while QDOH is not. Although there have been a few surface-modified CdS nanoclusters that are soluble in various low-boiling solvents,[14] these data further demonstrate that nanocluster solubility is highly dependent on the nature of the surface functionality.

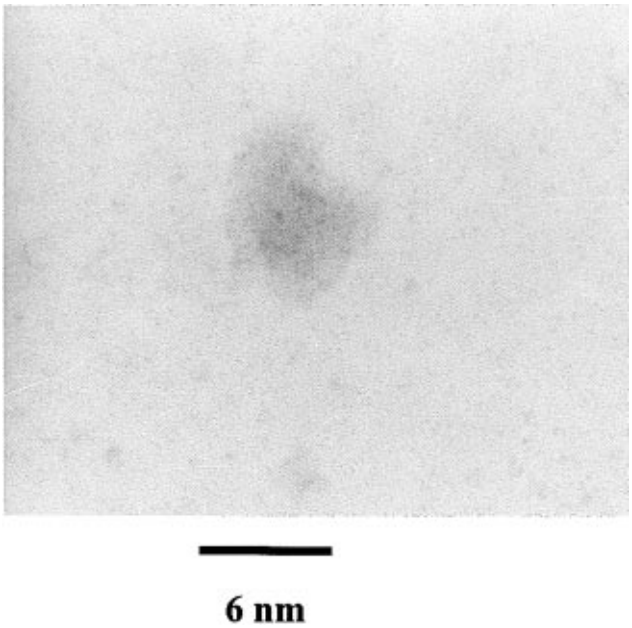

Figure 6. Transmission electron micrograph of a dried QDOH suspension ($CHCl_3$) on a carbon-coated copper grid. Magnification: 290 000×.

Conclusions

Quantum-confined semiconductor nanoclusters, or quantum dots, represent an exciting new class of electronic materials with potential device activity. The realization of novel molecular electronic devices fabricated from quantum dots necessitates the activation of the cluster surface toward the covalent tethering of molecular moieties. We have been investigating the functionalization of cadmium sulfide quantum dots for such purposes, and report here the formation of a 30 Å diameter CdS nanocluster having a chemically active phenolic surface. We also demonstrate that the surface is receptive to covalent attachment of a variety of molecular fragments via esterification, and we describe a general method for enacting the esterification while maintaining the integrity of the cluster. We further demonstrate that the surface derivatives can be used to dramatically alter the solubility properties of CdS nanoclusters.

Acknowledgment. The authors are indebted to Professor A. B. P. Lever, Dr. H. Perez, Robert Suchozak (Dalton Chemical Company), Charles Chamchoumis, Ryan Margau, Robert Pestrin, Linda Pugliese, and Josie Galloro for their helpful comments and suggestions and to Mary Lou Ashton for her assistance with the electron microscopy. We also wish to thank the Natural Sciences and Engineering Research Council of Canada (NSERC) for their financial support.

CM970189M

(13) (a) Wang, Y.; Herron, N. *Phys. Rev. B* **1990**, *42*, 7253. (b) Wang, Y.; Herron, N. *J. Phys. Chem.* **1991**, *95*, 525. (c) Vossmeyer, T.; Katsikas, L.; Giersig, M.; Popovic, I. G.; Diesner, K.; Chemsddine, A.; Eychmüller, A.; Weller, H. *J. Phys. Chem.* **1994**, *98*, 7665.

(14) (a) Colvin, V. L.; Goldstein, A. N.; Alivisatos, A. P. *J. Am. Chem. Soc.* **1992**, *114*, 5221. (b) Herron, N.; Wang, Y.; Eckert, H. *J. Am. Chem. Soc.* **1990**, *112*, 1322. (c) Ogata, T.; Hosokawa, H.; Tatsuhiko, O.; Wada, Y.; Sakata, T.; Mori, H.; Yanagida, S. *Chem. Lett.* **1992**, 1665.

(15) This reported precision is limited by the resolution of the microscope.